PLOS ONE

RESEARCH ARTICLE

Infection model of THP-1 cells, growth dynamics, and antimicrobial susceptibility of clinical *Mycobacterium abscessus* isolates from cystic fibrosis patients: Results from a multicentre study

Alba Ruedas-López[1,2], Marta Tato[3], Laura Lerma[2], Jaime Esteban[2,4,5], María-Carmen Muñoz-Egea[4,5], Carlos Toro[6], Diego Domingo[7], Rafael Prados-Rosales[2☯*], Paula López-Roa[1☯*]

1 Clinical Microbiology and Parasitology Department, Hospital Universitario 12 de Octubre, Madrid, Spain, **2** Department of Preventive Medicine, Public Health and Microbiology, School of Medicine, Universidad Autónoma de Madrid, Madrid, Spain, **3** Clinical Microbiology and Parasitology Department, Hospital Universitario Ramón y Cajal, Madrid, Spain, **4** .Clinical Microbiology Department, IIS-Fundación Jiménez Díaz, UAM. Madrid, Spain, **5** CIBERINFEC-CIBER de Enfermedades Infecciosas, Madrid, Spain, **6** Clinical Microbiology and Parasitology Department, Hospital Universitario La Paz, Madrid, Spain, **7** Clinical Microbiology and Parasitology Department, Hospital Universitario de La Princesa, Madrid, Spain

☯ These authors contributed equally to this work and share corresponding authorship.
* plroa@salud.madrid.org (PL-R); rafael.prados@uam.es (RP-R)

OPEN ACCESS

Citation: Ruedas-López A, Tato M, Lerma L, Esteban J, Muñoz-Egea M-C, Toro C, et al. (2025) Infection model of THP-1 cells, growth dynamics, and antimicrobial susceptibility of clinical Mycobacterium abscessus isolates from cystic fibrosis patients: Results from a multicentre study. PLoS ONE 20(3): e0319710. https://doi.org/10.1371/journal.pone.0319710

Editor: Thomas Byrd, The University of New Mexico School of Medicine, UNITED STATES OF AMERICA

Received: October 24, 2024

Accepted: February 5, 2025

Published: March 31, 2025

Data availability statement: The data that support the findings of this study are openly available in Figshare. The data can be accessed at Figshare using the following DOI links: https://doi.org/10.6084/m9.figshare.28398944.v1 https://doi.org/10.6084/m9.figshare.28398398.

Abstract

Mycobacterium abscessus (MABS) is an emerging pathogen causing severe infections, particularly in cystic fibrosis (CF) patients. A prospective multicentre study included CF patients from four hospitals in Madrid between January 2022 and January 2024. Respiratory samples were collected, and MABS isolates were analysed to determine their antibiotic resistance profiles, growth dynamics, infection kinetics, intracellular behaviour, and pathogenicity. Intracellular bacterial growth and macrophage viability were evaluated through THP-1 cell infection experiments, with and without amikacin. Phenotypic susceptibility testing and genotypic susceptibility testing were also conducted. Among 148 patients, 28 MABS isolates were detected from 16 patients (10.8%), and the first isolate from each patient was analysed. Isolation was more prevalent in younger individuals (median age 24.4 vs. 28.4 years, p = 0.049), and most isolates (81.25%) were identified as *M. abscessus subsp. abscessus* (MABSa). MABS isolates exhibited high resistance rates (>85%) to doxycycline, tobramycin, ciprofloxacin, moxifloxacin (75%) and cotrimoxazole (56.3%). Amikacin resistance (18.8%) was higher than expected, and inducible (10/16 isolates) or acquired (1/16 isolate) macrolide resistance was found in 68.8% of strains. Phenotypic and genotypic testing results were fully concordant. Tigecycline demonstrated strong *in vitro* activity, and resistance to imipenem, linezolid, and cefoxitin remained low. Rough strains displayed lower optical density values in later growth stages, probably due to their increased aggregation. In THP-1 cell infection experiments, rough strains showed higher intracellular bacterial loads with statistically significant differences observed at 2

v1 https://doi.org/10.6084/m9.figshare.28398227.v2 https://doi.org/10.6084/m9.figshare.28398899.v1 https://doi.org/10.6084/m9.figshare.28398275.v2

Funding: Author: PLR Grant Number: PI21/01738 Funder: Instituto de Salud Carlos III (ISCIII), co-funded by the European Union Funder URL: www.isciii.es Author: RPR Funding Contracts: NIH RO1AI162821, PID2019-110240RB-I00, PID2022-136611OB-I00 Funders: National Institutes of Health (NIH) and Spanish Ministry of Science and Innovation (MICINN) Funder URLs: www.nih.gov and www.ciencia.gob.es The funders did not play any role in the study design, data collection and analysis, decision to publish, or preparation of the manuscript.

Competing interests: The authors have declared that no competing interests exist.

hours (both with and without amikacin) and at 72 hours (with amikacin) post infection. Notably, rough strains also exhibited a higher internalisation index and greater impact on THP-1 cell viability, especially in the absence of amikacin.

Introduction

Mycobacterium abscessus (MABS) is a rapidly growing non-tuberculous Mycobacteria (RG-NTM) responsible for soft tissue [1] and wound infections [2], as well as progressive pulmonary diseases [3,4]. MABS has increasingly been recognised as an emerging pathogen, especially in patients with chronic lung conditions such as Cystic Fibrosis (CF) [5,6]. This species is classified into three subspecies: *M. abscessus subsp. abscessus* (MABSa), *M. abscessus subsp. massiliense* (MABSm) and *M. abscessus subsp. bolletii* (MABSb) [7]. Clinically, this distinction is crucial, as MABSa and MABSb typically show inducible macrolide resistance due to the *erm*(41) gene, whereas MABSm, with a truncated *erm*(41), remains susceptible to macrolides [8] in the absence of other resistance mechanisms. Furthermore, MABS is able to promote immune evasion, persistent infections [9–11], and resistance to diverse antibiotics [12], representing a complex challenge in the treatment of CF patients [6]. MABS strains exhibit distinct colony morphologies when cultured on solid media. Rough (R) colonies are characterised by a dry and irregular surface with numerous crests and folds, while smooth (S) colonies display a uniform, shiny, and moisty appearance [13,14]. The R morphotype, which lacks glycopeptidolipids (GPL) in its cell wall, is associated with pronounced bacterial clumping and the formation of cord-like structures [15]. This feature has been linked to increased virulence in *in vitro* studies [13], animal models [13,16] and humans [17]. The aggregation phenomenon complicates the accurate measurement of optical density (OD) and its correlation with colony-forming units (CFU). This challenge is significant as the CFU-OD relationship is vital for preparing bacterial inocula of known concentration for subsequent *in vitro* experiments.

THP-1 cells, derived from human monocytic leukaemia [18], serve as a model to study macrophage responses to infections. Previous studies have shown that MABS isolates with high virulence in other models, such as the silkworm infection model, also exhibit increased cytotoxicity to human THP-1-derived macrophages [19]. Differentiated THP-1 cells mimic human macrophages, providing a valuable system for investigating the intracellular behaviour, virulence and intracellular drug testing of pathogens such as MABS [20,21].

Here, we sought to characterise the growth dynamics, virulence, and antimicrobial susceptibility of MABS clinical strains. We aimed to investigate potential differences in the infection kinetics of these clinical MABS strains within THP-1 cells by evaluating their internalisation and proliferation capacities and their ability to impact THP-1 cell viability. Additionally, we sought to optimise and identify the limitations of the methodologies employed, including the assessment of the impact of amikacin on infection experiments.

Materials and methods

Ethics statement

This study was conducted following the ethical principles of the Declaration of Helsinki and received approval from the Institutional Ethics Committee of Hospital 12 de Octubre (reference number: CEIm 21/592), ensuring compliance with international ethical standards. All procedures adhered to hospital biosafety regulations and were approved by the Local Institutional Review Board. Written informed consent was obtained from all participants.

Study design and data collection

Following approval from our Local Institutional Review Board, we conducted a prospective multicentre study including patients from four tertiary hospitals with CF units in Madrid. The recruitment period extended from January 1, 2022, to April 30, 2023. The study protocol entailed an initial baseline visit (month 0), followed by three visits at three-month intervals (months 3, 6, and 9), an annual visit (month 12), and a final visit at two years, which has not yet been completed for most patients. During the follow-up visits, respiratory samples were obtained, and clinical and microbiological data were collected and managed using REDCap (Research Electronic Data Capture) tools [22]. The bacterial strains included in the study were those isolated during the visits conducted between January 1, 2022, and January 1, 2024.

Phenotypic and genotypic susceptibility testing

Phenotypic and genotypic susceptibility testing were performed as described previously [23]. Briefly, phenotypic antimicrobial resistance was assessed using the broth microdilution method with RAPMYCOI Sensititre™ titration plates, following CLSI standard M24 document [24]. The antibiotics tested included cotrimoxazole, ciprofloxacin, moxifloxacin, cefoxitin, amikacin, doxycycline, tigecycline, clarithromycin, linezolid, imipenem, and tobramycin. Genotypic susceptibility testing involved the GenoLyse® DNA extraction kit and GenoType® Mycobacterium NTM-DR test to identify MABS subspecies and resistance mutations in the *erm(41), rrl*, and *rrs* genes.

Bacterial strains and growth conditions

Clinical and the laboratory ATCC 19977 reference [25] strains were grown in 10 mL of liquid Middlebrook 7H9 broth (Difco, BD Bioscience) in 25 mL untreated tissue culture flasks (Glass Chemicals, Spain), supplemented with 10% Middlebrook OADC (oleic acid-albumin-extrose-catalase; BBL, Becton-Dickinson), 0.2% glycerol, and 0.5% Tween 80 at 37°C with shaking at 200 rpm.

Preparation of bacterial inoculum for subsequent infection of THP-1 cells

Bacterial inocula were prepared using two different methods. (i) Bacteria were initially collected at the logarithmic phase, centrifuged at 5000 × g for 10 minutes, and washed three times in phosphate-buffered saline (PBS). To prevent clumping, the liquid cultures were consistently passed 10 times through a syringe with a 25G-needle and vortexed with 4 mm glass beads for 10 seconds. The bacterial suspension was diluted in PBS to an OD of approximately 1, and the exact OD was measured at 600 nm using a BioPhotometer Plus® spectrophotometer (Eppendorf AG, Germany). Viable counts were obtained by plating serial dilutions on Columbia + 5% sheep blood agar plates (bioMérieux, France), followed by incubation at 37°C for one week. This procedure allowed us to calculate the CFU/OD ratio for each strain, however this procedure was not robust enough (see results section). (ii) Alternatively, aliquots of bacterial suspensions were stored at -80 ºC and used for further infections. Three aliquots of each strain were thawed one week after preparation, and the number of microorganisms was evaluated by plating 10-fold dilutions of the bacterial suspension. The remaining aliquots were kept frozen at − 80 °C until required. This procedure enabled us to determine the precise concentration (CFU/mL) for each frozen strain.

Growth curves and doubling time calculations

To study the growth kinetics and doubling times of clinical isolates, we set up precultures from frozen stocks that, after 24 h, were reinoculated in fresh medium adjusting OD to 0.01 (time

0). Subsequently, OD was measured every 24-h for 5 days and viable counts were obtained by plating serial dilutions at 24 and 48 hours. The bacterial doubling time (BDT) was calculated using the following formula: $BDT = t * ln(2)/ ln(N(final\ time)/ N(initial\ time))$, where *N(final time)* is CFU/mL at 48 hours, *N(initial time)* is CFU/mL at 24 hours, and *t* is 24 hours *(final time* (48h) – *initial time* (24h)).

Infection of THP-1 cells

THP-1 cells were cultured in 75 cm^2 flasks in complete medium (CM): RPMI medium (Gibco™, Thermo Fisher Scientific, USA) supplemented with 10% heat-inactivated fetal bovine serum (FBS, Biowest, France), 100 U/mL penicillin, 100 μg/mL streptomycin and 50 μg/mL gentamycin (Gibco™, Thermo Fisher Scientific, USA) at 37 °C and 5% CO_2. To differentiate THP-1 monocytes into macrophage-like cells, cells were treated with 50 ng/mL of phorbol 12-myristate 13-acetate (PMA), seeded at 10^5 cells/well in 96-well plates (Nunc™ MicroWell™ 96-Well, Thermo Fisher Scientific, USA) and incubated for 72h. Following CM removal, the monolayers were washed with Dulbecco's PBS (dPBS, Gibco™, Thermo Fisher Scientific, USA) and infected at a multiplicity of infection (MOI) of 1.

Bacterial inocula were prepared by first collecting cells at mid -logarithmic phase by centrifuging at 5000 × g for 10 minutes and washing three times with PBS. The OD was then adjusted in RPMI supplemented with 10% non-inactivated FBS and without antibiotics (incomplete medium, IM), to achieve a concentration of 10^6 CFU/mL, based on the previously calculated CFU-OD ratio for each strain. Additionally, bacterial inocula were prepared by adding the necessary microliters from each previously frozen aliquot to IM, achieving a concentration of 10^6 bacteria/mL. Thus, adding 100 μ L of these preparations provided 10^5 bacteria per well. To confirm that the correct inoculum was added, all inocula used for infection experiments were plated and CFUs were counted. Then, infection was left to progress for 2 hours. Non-infected control macrophages received only IM, and all experiments were prepared in triplicate. Further, macrophages were washed three times in dPBS to remove extracellular bacteria and either treated or not with amikacin (250 μg/mL) for 1 h. Further, cells were washed again three times in dPBS and subsequently maintained in IM with or without 50 μg/mL amikacin for the duration of the experiment. To ensure consistency across both methodologies and maintain the same number of washes, cells were washed three times in dPBS, and the medium was replaced every 24 hours.

Quantification of intracellular bacterial growth

To enumerate intracellular bacterial cells, infected THP-1 cells were washed with dPBS at each post-infection time to remove any residual amikacin (which could inhibit bacterial growth on solid media) and to eliminate any remaining extracellular bacteria and lysed in PBS containing 0.1% Triton X-100. After 5 minutes, bacterial suspensions and cell debris were serially diluted and plated on Columbia + 5% sheep blood agar plates.

THP-1 viability measurements

For THP-1 viability experiments, infected monolayers were washed as above and treated with dPBS containing 2 mM Carboxyfluorescein diacetate succinimidyl ester (CFDA-SE Cell Proliferation Assay Kit, Bio-Rad) at room temperature (RT) for 15 minutes, washed three times with dPBS, and imaged using the EVOS FL (Thermo Fisher Scientific, Waltham, MA, USA) fluorescence microscope. Images were captured from three different fields of each well, and cell counting was performed using ImageJ software [26].

Statistical analysis

Qualitative variables were presented with their frequency distributions (e.g., gender, MABS isolation). The association between qualitative variables (MABS isolation vs. sex) was evaluated using Fisher's exact test because more than 20% of the expected values were less than 5.

Quantitative variables were reported with their mean value and standard deviation (SD) or Confidence Interval of 95% (CI 95%) when the data followed a normal distribution, and with median and interquartile range (IQR) when the data were not normally distributed. The Shapiro-Wilk test was used to assess whether the data followed a normal distribution, and the non-parametric Mann-Whitney U test was employed to compare age distributions between groups (with MABS isolates vs. without MABS isolates), due to the deviation from normality in the MABS isolation group. When data followed a normal distribution, t-tests were employed. Student´s-test for inequal variances (Welch's test) was employed when Levene's test indicated unequal variances, while Student's t-test was used when variances were equal.

One-way ANOVA and two-way ANOVA, with adjustments for sphericity using the Geisser-Greenhouse correction, followed by Dunnett's post hoc test, were used to analyse the results of the internalisation and THP-1 viability experiments.

A significance value of 5% was accepted for all tests. Statistical analyses were performed with Stata 17.0 and GraphPad Prism 8.3.

Results

Prevalence and clinical features of *M. abscessus* in the Spanish cohort

The study included 148 patients with CF. To date, 28 isolates of MABS have been found from 16 different patients, resulting in a prevalence of 10.8%. Among these patients, eight (5.4%) had one isolate, four (2.7%) had two isolates, and another four (2.7%) had three isolates. In this preliminary study, only the first isolate from each patient was stored for further analyses.

Among the 148 patients, 81 were men (54.7%). The mean age was 29.3 (SD = 13.9) and 29.6 (SD = 13.8) years for men and women, respectively. The median age of patients with MABS isolates was 24.4 years (IQR: 15.9-28.9) compared to 28.6 years (IQR: 20.8-38.3) for patients without MABS isolates, (p = 0.049). Regarding sex, 75.0% (12/16) of the patients with MABS isolation were male, compared to 52.3% (69/132) in the group without MABS isolation. The association between sex and MABS isolation was not statistically significant (p = 0.1) (Table 1).

Out of 16 MABS clinical isolates, 13 (81.25%) were identified as MABSa and 3 (18.75%) as MABSm (strains 2, 8 and 16). No isolates of MABSb were found.

Regarding morphology, eight strains were initially classified as R and another eight as S morphotypes. However, in subsequent experiments, a small proportion of R colonies was observed in strains 4 and 14, initially classified as S. Nevertheless, due to the predominance

Table 1. Age and sex distribution of CF patients by MABS culture results.

	MABS culture		
	Negative	**Positive**	**p-value**
Age Median (IQR)	28.6 (20.9-38.3)	24.4 (15.9-28.9)	0.049 [a]
Male N (%)	69 (52.3%)	12 (75.0)	0.1[b]
Female N (%)	63 (47.7)	4 (25.0)	

[a]Mann-Whitney U test, exact p-value.

[b]Fisher's exact test.

https://doi.org/10.1371/journal.pone.0319710.t001

of S colonies during the experiments, these strains were analysed within the S group. Specifically, we found that 50% (8/16) were R, 37.5% (6/16) of the isolates were S, and 12.5% (2/16) exhibited a mixed morphology. Fig 1 shows an example of the phenotypic characteristics of colonies from each morphotype.

Phenotypic and genotypic susceptibility testing

Table 2 summarises the distribution and interpretation of Minimum Inhibitory Concentrations (MICs) by subspecies. The highest *in vitro* resistance rates among MABS isolates were observed for doxycycline (100.0%), tobramycin (87.5%), ciprofloxacin (87.5%), moxifloxacin (75.0%), and cotrimoxazole (56.3%). In contrast, isolates demonstrated lower resistance rates to amikacin (18.8%), imipenem (12.5%), linezolid (6.3%), and cefoxitin (0.0%). Among MABSa isolates, 10 out of 13 exhibited inducible resistance to clarithromycin, while the remaining three, harbouring the T28C polymorphism in the *erm(41)* gene, remained susceptible after 14 days of incubation. Only one isolate (MABSm) demonstrated acquired resistance to clarithromycin, carrying a mutation in the *rrl* gene at position A2058G, as identified by the GenoType® test. Regarding amikacin resistance, 3 out of 16 isolates showed *in vitro* resistance: one belonged to the MABSm subspecies (strain number 16) and the other two to the MABSa subspecies (strains numbers 9 and 13). The GenoType® test detected mutations in the *rrs* gene in all these resistant strains. There was a 100% concordance between the GenoType® test results and phenotypic susceptibility testing across all studied genes (*erm(41), rrl,* and *rrs*), with all 16 isolates showing consistent results.

Growth curves measured by OD, determination of CFU/OD and CFU/mL relationship, and doubling time

We initially monitored the growth by measuring OD and found differences between isolates displaying different morphotypes (Fig 2, Table 3). We noted that strains from both morphotypes followed a similar growth dynamic. However, S strains reached higher OD values compared to R strains. Specifically, no significant differences in OD were observed between the morphotypes at 24 h. Moreover, S strains consistently exhibited significantly higher OD values

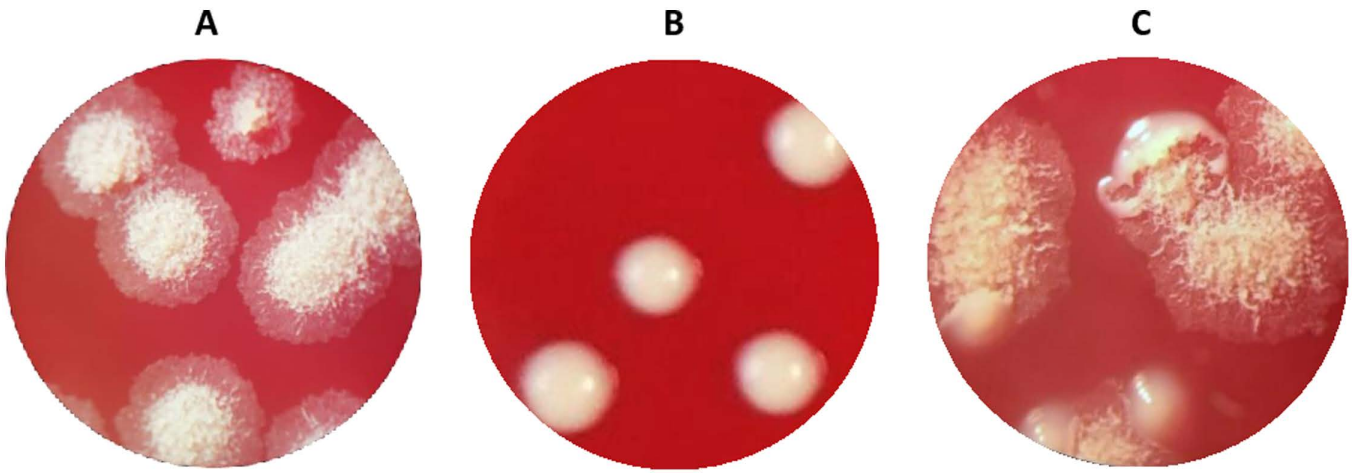

Fig 1. Example of morphotypes: A rough; B: smooth; C: mixed (strain 14).

https://doi.org/10.1371/journal.pone.0319710.g001

Table 2. Antimicrobial susceptibility testing of MABS isolates.

Drug Subsp.	Number of strains at each MIC (μg/mL)												N(%) Resistant
	≤0.06	**0.12**	**0.25**	**0.5**	**1**	**2**	**4**	**8**	**16**	**32**	**64**	**128**	
Cotrimoxazole													
MABSa (n=13)			1		1	2			9[↑]				9 (69.2)
MABSm (n=3)						3							0 (0.0)
Ciprofloxacin													
MABSa						1[*]	4	8[↑]					12 (92.3)
MABSm				1				2[↑]					2 (66.7)
Moxifloxacin													
MABSa					1	2[*]	2		8[↑]				10 (76.9)
MABSm					1		2						2 (66.7)
Cefoxitin													
MABSa								1	8	4[*]			0 (0.0)
MABSm									2	1[*]			0 (0.0)
Tigecycline [¥]													
MABSa	*2*	*3*	*6*	*2*									¥
MABSm	*1*	*2*											¥
Amikacin													
MABSa							3	4	4			2[↑,a]	2 (15.4)
MABSm							2					1[↑,a]	1 (33.3)
Drug Subsp.	Number of strains at each MIC (μg/ml)												
	≤0.06	0.12	0.25	0.5	1	2	4	8	16	32	64	128	
Clarithromycin (3 days)													
MABSa	5		2	4	2								0 (0.0)
MABSm	2									1[↑,b]			1 (33.0)
Clarithromycin (14 days)													
MABSa		2[c]			1[c]					10[↑]			10 (76.9)
MABSm[d]	1	1											0 (0.0)
Linezolid													
MABSa					2	2	1		7[*]		1[↑]		1 (7.7)
MABSm					1		2						0 (0.0)
Imipenem													
MABSa							4	3[*]	5[*]	1			1 (7.7)
MABSm								2[*]				1[↑]	1 (33.3)
Tobramycin													
MABSa						1	1[*]	3	7	1[↑]			11 (84.6)
xMABSm								1	2				3 (100.0)

Strains with MICs interpreted as **Resistant** are highlighted in **bold**.

[*]Indicates strains with MICs interpreted as Intermediate.

[¥]No established breakpoints exist for tigecycline; the number of strains at each MIC is shown in *italic* type.

[↑]Off-scale high MICs were included at the next highest concentration.

[a]Strains harbouring a *rrs* mutation.

[b]MABSm strain harbouring a *rrl* mutation (acquired resistance to clarithromycin).

[c]Strains harbouring the T28C mutation at *erm(41),* not showing inducible resistance.

[d]MABSm strain showing acquired resistance to clarithromycin was excluded from this analysis.

https://doi.org/10.1371/journal.pone.0319710.t002

compared to R strains at 48, 72, 96, and 120 hours. In both morphotypes, the mid-logarithmic phase was registered between 24 and 48 hours.

Aiming at establishing an OD-CFU ratio we plated cultures from each strain at different time points and found that this approach does not provide consistent results being not reliable for further studies. Specifically, we adjusted 24 and 48-h cultures to an OD = 1 (CFU-OD = 1) performed serial dilutions and plated them in solid medium. We observed that the CFU-OD = 1 ratio was significantly higher at 48 hours compared to 24 hours for both morphotypes. While the CFU-OD = 1 ratio is similar between morphotypes at 24 hours, it increases approximately 10-fold for the R strains at 48 hours (Table 4). Importantly, when we performed this procedure to infect the cells, we found that this ratio was not robust enough to accurately adjust the initial bacterial inoculum to 10^6 bacteria/mL, resulting these inocula in a

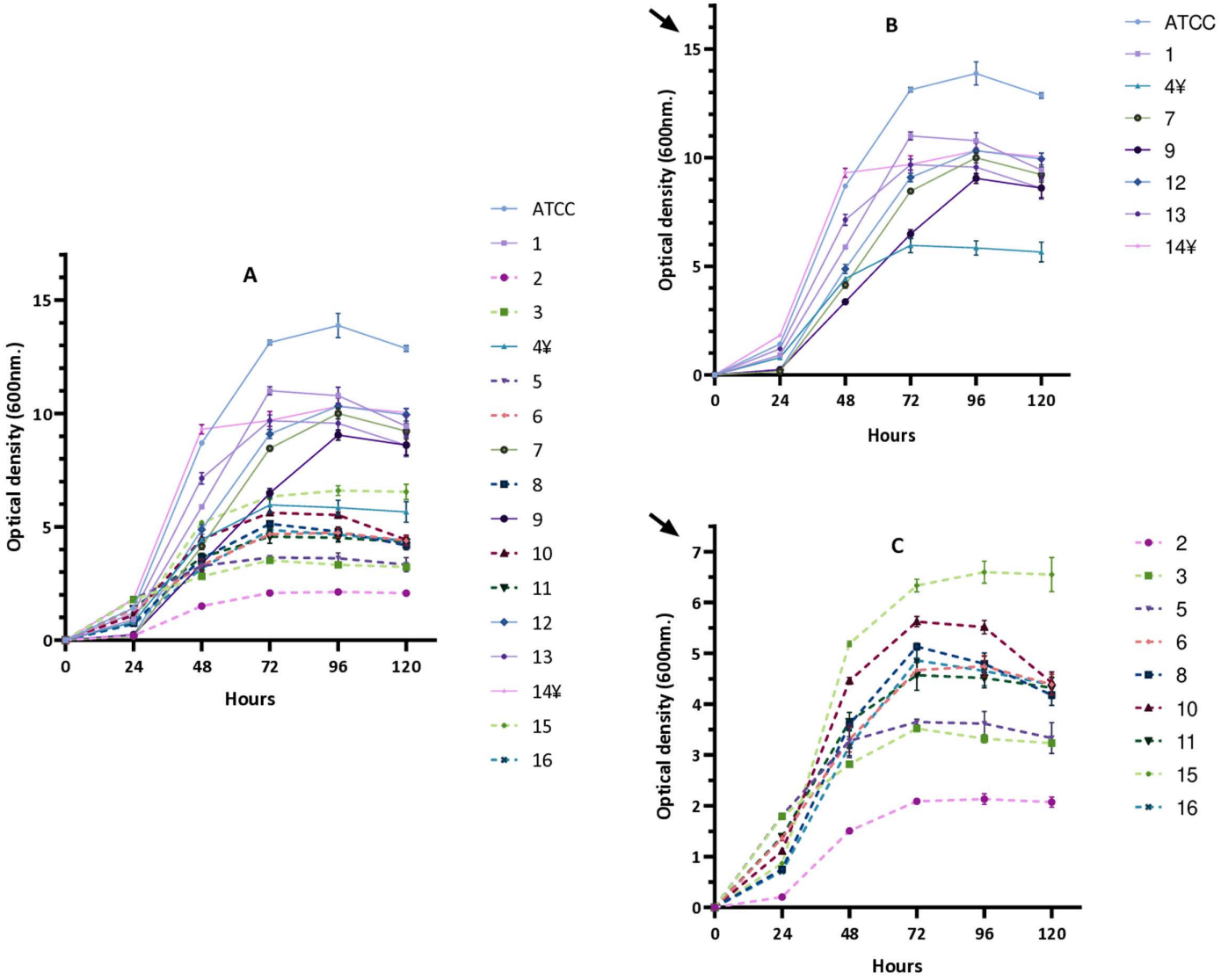

Fig 2. Growth dynamics of smooth and rough strains over time by measuring OD. Panel A represents data for all strains**. B:** smooth strains**; C:** rough strains with rescaled OD values (see arrows). Although smooth (**B**) and rough (**C**) strains manifested similar growth dynamics, smooth strains reached higher OD values. Data are mean and SD from three independent experiments.

https://doi.org/10.1371/journal.pone.0319710.g002

median of 7.2×10^5 CFU/mL (range: $1.1 \times 10^4 - 1.2 \times 10^7$). To circumvent this, we evaluated whether freezing aliquots of these bacterial suspensions at -80°C could be a reliable method to calculate the CFU/mL ratio. This approach proved to be much accurate in achieving a known bacterial inoculum concentration for subsequent THP-1 infections, with a median of 9.9×10^5 CFU/mL (range: $7.5 \times 10^5 - 1.3 \times 10^6$). Therefore, all subsequent experiments requiring a known bacterial inoculum such as THP-1 infection and viability assays, were performed using this CFU/mL procedure, which involved freezing aliquots.

Regarding the bacterial doubling time, calculated using the formula "*BDT = t * ln(2)/ ln(N(final time)/ N(initial time))",* no significant differences were observed between S strains (5.3 hours, 95% CI: 4.7-5.9) and R strains (5.5 hours, 95% CI: 5.0-6.0), p = 0.6. (S1 Table).

Quantification of intracellular MABS survival in THP-1 cells

Using THP-1 cells as a model, we initially investigated the internalisation indices for each strain by counting the internalised bacterial cells 2 h after infection. A significantly higher internalisation index mean was observed for the R morphotypes (26.4% ± 7.1%) compared to the S morphotypes (12.4% ± 8.8%), p = 0.003 (Fig 3). We noted that strains 4 and 14, which manifested a mixed morphology, showed internalisation indices similar to that of R strains. Conversely, R strain 8 exhibited a notably low internalisation index compared to other R strains.

Subsequently, we explored the intracellular survival of MABS isolates in a time course experiment. We found that throughout the infection experiments R strains exhibited higher mean bacterial numbers compared to S strains at all time points and conditions evaluated.

Table 3. Optical density results at each time point, compared by morphology.

S strains				R strains			Difference in means
Hours	**Mean-OD**	**SD [a]**	**CI 95%**	**Mean-OD**	**SD [a]**	**CI 95%**	
24	0.85	0.61	0.34-1.36	1.11	0.53	0.70-1.52	-0.26^{ns}
48	5.98	2.19	4.15-7.81	3.44	1.02	2.65-4.23	2.54*
72	9.19	2.32	7.25-11.14	4.49	1.26	3.53-5.46	4.70**
96	9.97	2.21	8.11-11.82	4.43	1.29	3.43-5.42	5.53**
120	9.30	2.00	7.63-10.97	4.10	1.21	3.16-5.03	5.20**

Student's t-test.

$^{*}p < 0.05$.

$^{**}p < 0.001$.

[a]Standard deviation

https://doi.org/10.1371/journal.pone.0319710.t003

Table 4. CFU-OD = 1 ratio at 24 and 48 hpi, compared by morphology.

	S strains		R strains			
Hours	**CFU-OD = 1**	**SD**	**CFU-OD = 1**	**SD**	**p-value [a]**	**Prob.(R > S) [b]**
24	1.18e + 09	5.64e + 08	1.63e + 09	1.56e + 09	0.70	0.56
48	3.52e + 09	2.33e + 09	1.11e + 10	1.24e + 10	**0.02**	0.83
p-value-(column)[a]	**0.03**		**<0.001**			
P(48h > 24h)[b]	0.83		0.95			

[a]Mann-Whitney U test, exact p-value;

[b]Probability of superiority.

https://doi.org/10.1371/journal.pone.0319710.t004

Importantly, amikacin is typically used in these experiments to prevent the proliferation of extracellular bacteria, and it has been shown that does not penetrate inside THP-1 cells [27]. In this context, amikacin-resistant strains (strains 9, 13 and 16) were excluded when this antibiotic was used during experimental infections, except at 2 hours post-infection (hpi). When cells were maintained in medium with amikacin throughout the infection experiment, significant differences were observed in the mean number of intracellular MABS between S and R strains at 2 hpi, with R strains showing higher cell counts ($2.4x10^5 \pm 1.2 \times 10^5$ CFU/mL) compared to S strains ($1.1x10^5 \pm 9.6x10^4$ CFU/mL), $p = 0.02$. However, these differences disappeared at 24, 48 and 72 hpi ($p = 0.05$; $p = 0.5$; $p = 0.4$, respectively). These analyses compare the mean values of S and R strains, based on individual data shown in Fig 4C and 4D. Conversely, when amikacin was not included in the medium after infection, significant differences were observed at 2 hpi, with R strains showing higher cell counts ($3.1 \times 10^5 \pm 1.8 \times 10^5$CFU/mL) compared to S strains ($1.3x10^5 \pm 6.4x10^4$ CFU/mL), $p = 0.02$. Similarly, R strains also exhibited higher CFU/mL means compared to S strains at 24 and 48 hpi, but these differences were not statistically significant ($p = 0.05$ and $p = 0.06$, respectively). However, bacterial loads were

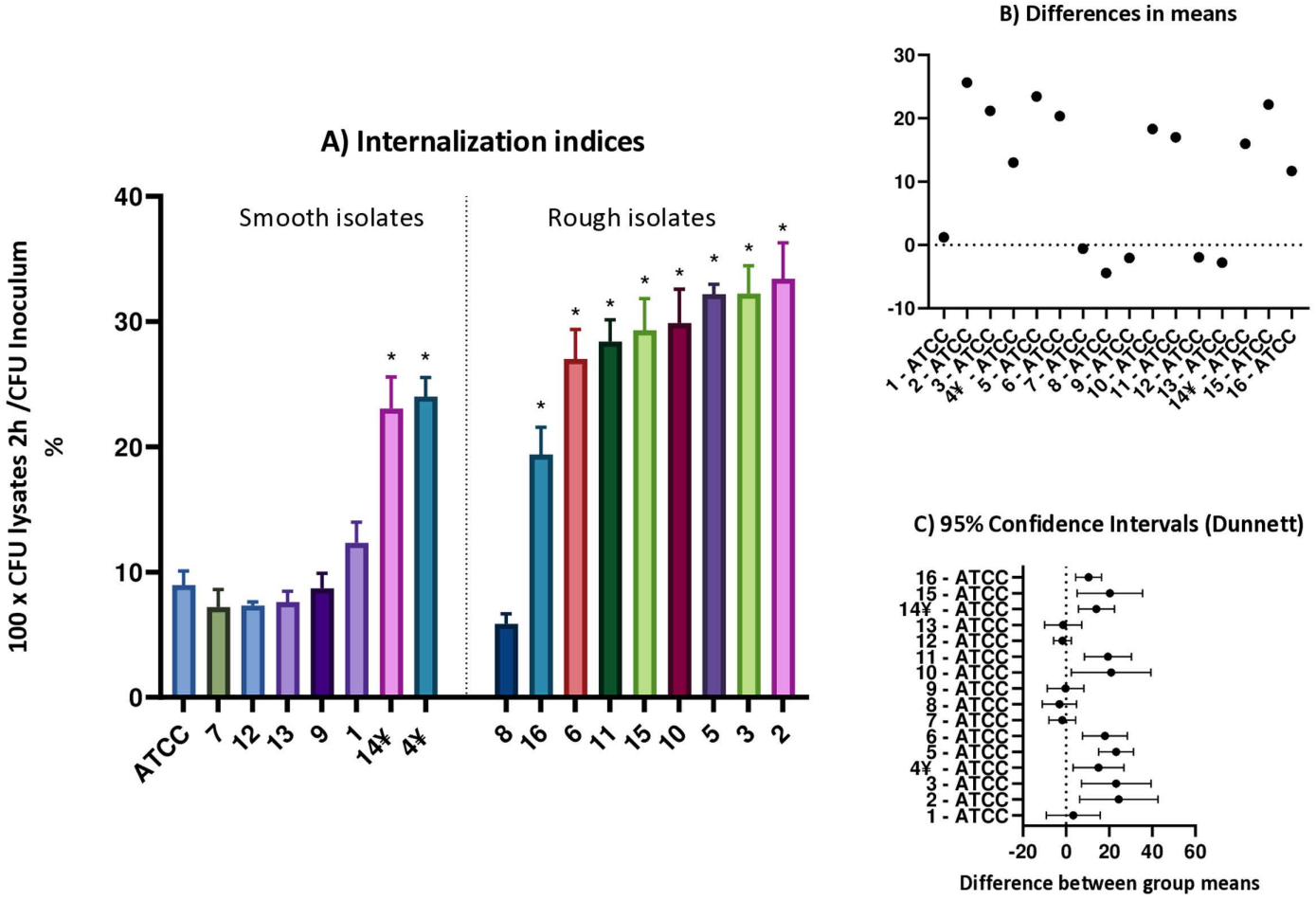

Fig 3. Internalisation indices for each MABS strain, compared with the ATCC strain. A: Error bars indicate the SD, based on the results from three independent experiments. * $p < 0.05$. One-way ANOVA with Dunnett's post hoc test. B: Differences in means for internalisation indices, comparing each strain to the ATCC strain. C: 95% confidence intervals for the differences in group means, using Dunnett's method for multiple comparisons. ¥ Strains exhibiting mixed morphology.

https://doi.org/10.1371/journal.pone.0319710.g003

significantly higher in R strains ($4.0 \times 10^7 \pm 9.4 \times 10^6$ CFU/mL) at 72 hpi relative to S strains ($1.0 \times 10^7 \pm 3.4 \times 10^6$ CFU/mL), p = 0.01 (Fig 4A and 4B).

Viability of MABS-infected THP-1 cells

We next studied the viability of THP-1 cells after infection using a fluorescence dye. We found no significant differences in THP-1 cell viability between cells infected with S or R strains in the absence of amikacin at 2 and 24 hpi (Fig 5A, section "a" in S2 Table and S1B and S1C Fig. These differences were statistically significant at 48 and 72 hpi where R strains showed an enhanced capacity to reduce THP-1 viability relative to macrophages infected with S strains (Fig 5A, section "a" in S2 Table and S1B and S1C Fig. Conversely, we found no significant differences in cell viability between cells infected with S or R strains at any time point when amikacin was used (Fig 5B, section "b" in S2 Table and S1E and S1F Fig. More detailed information on the statistical analyses is provided in S2 Table.

When analysing the effect of individual strains on THP-1 cell viability (Fig 6), the two-way repeated measures ANOVA test revealed significant impacts from both the time and the

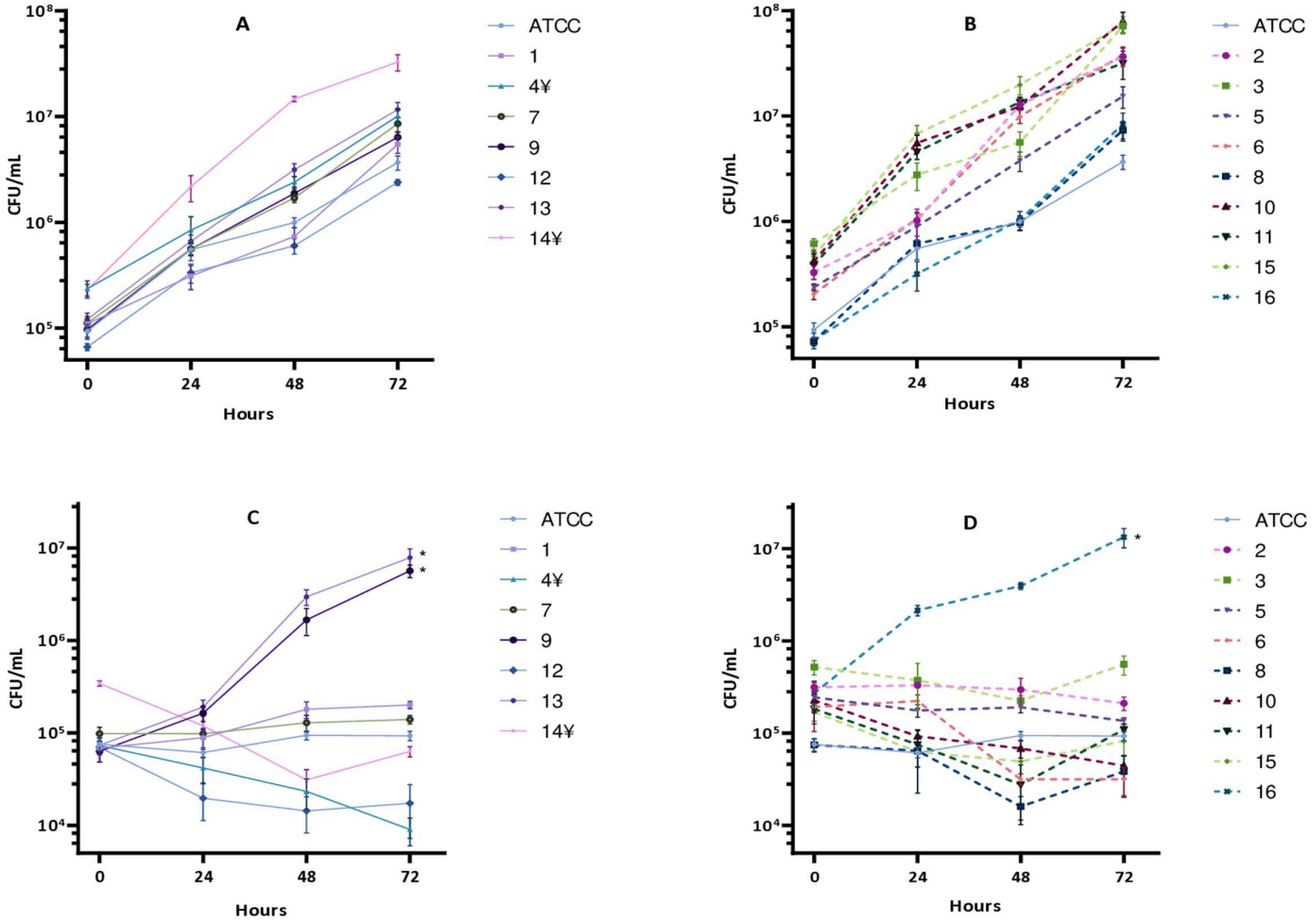

Fig 4. Intracellular growth of smooth and rough strains under amikacin or amikacin-free conditions. A, B: Intracellular growth of smooth and rough strains, respectively, in the absence of amikacin. C, D: Intracellular growth of smooth and rough strains, respectively, in the presence of amikacin. Error bars indicate the standard deviation, based on the results from three independent experiments. * Amikacin-resistant strains. ¥ Strains exhibiting mixed morphology.

https://doi.org/10.1371/journal.pone.0319710.g004

strain factor. In experiments conducted without amikacin (Fig 6A and 6B and S1A–S1C Fig, significant differences in THP-1 cell viability compared to uninfected controls were detected at 48 hpi, with further significant disparities noted at the final time point, and with R strains demonstrating more pronounced effects. In contrast, in experiments with amikacin (Fig 6C and 6D and S1E and S1F Fig, significant differences in THP-1 cell viability were first observed at the final time point. Viability data, together with intracellular CFU counts, are presented in S2 Fig, illustrating potential relationships between these parameters across different strains and time points.

Notably, we could observe multiple cord-like aggregates (Fig 7A and 7B) for most R strains despite numerous washes between time points and before staining the cells when amikacin was not included in the experiment. Quantitative assessment of extracellular CFUs under these conditions was not feasible due to the experimental limitations; however, the formation of these prominent aggregates provides qualitative evidence of significant extracellular growth.

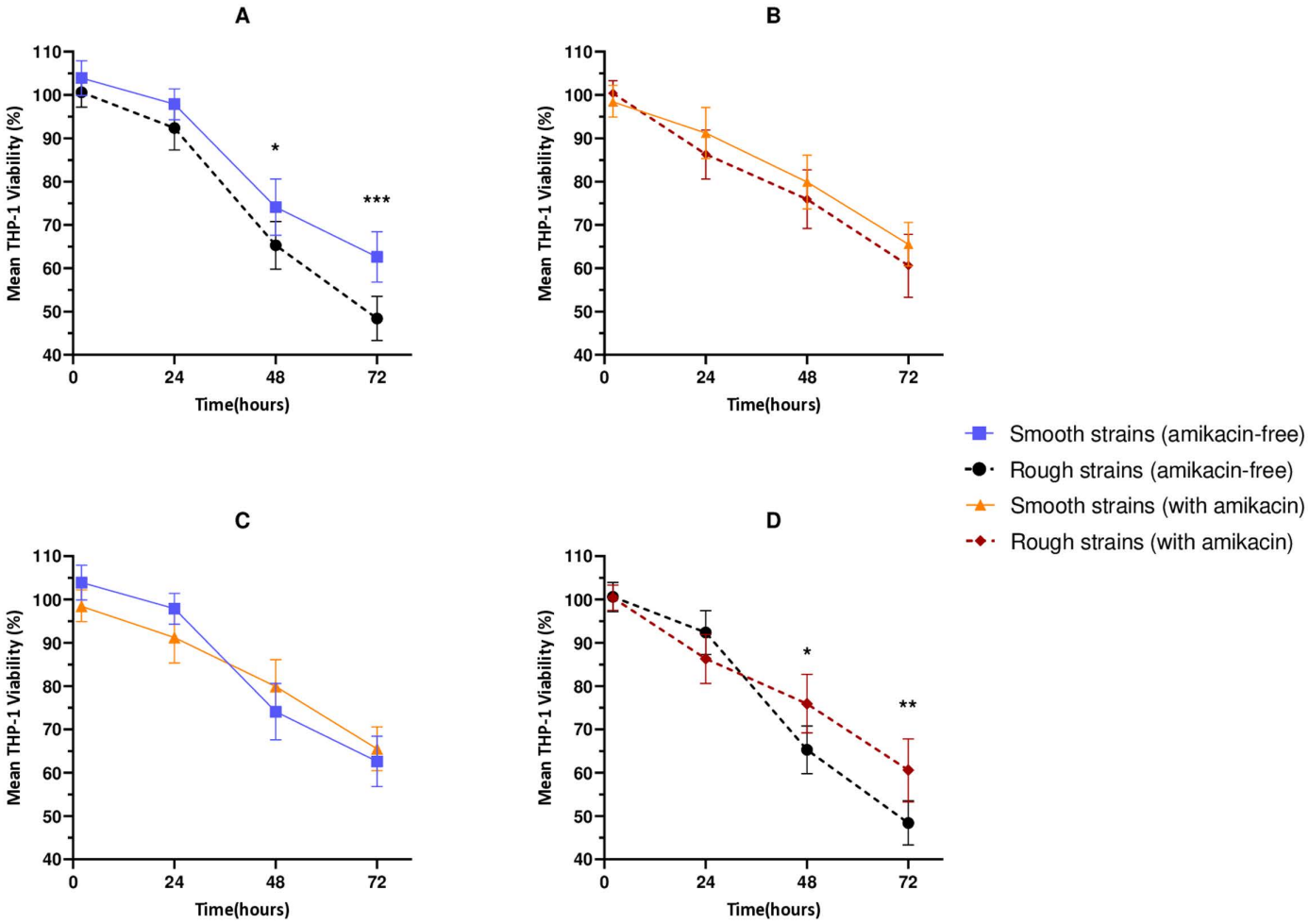

Fig 5. Effect of infection conditions on THP-1 cell viability. Data represent the mean ± 95% confidence interval of three independent experiments. Panels **A, B**: comparison of the viability of THP-1 cells infected with rough and smooth strains in amikacin-free medium (**A**) or amikacin-containing medium (B). Panels **C, D**: comparison of THP-1 cell viability in the absence or presence of amikacin for infections with **S (C)** and **R (D)** strains. Statistical significance was determined using a two-tailed Student's t-test. * **p** < 0.05; p < 0.01; ***p < 0.001.

https://doi.org/10.1371/journal.pone.0319710.g005

Finally, when comparing the effects of amikacin-containing medium versus amikacin-free medium on THP-1 cell viability, no significant differences were observed when THP-1 cells were infected with S at any time point. In contrast, for R strains, significant differences were observed at 48 and 72 hpi. Notably, we measured a mean viability of 65.3% (95% CI: 59.8 - 70.8,) without amikacin (section "a" in S2 Table, in bold) and 75.9% (95% CI: 69.2 - 82.6) with amikacin (section "b" in S2 Table, in bold) at 48 h, $p = 0.01$; and a mean viability of 48.4% (95% CI: 43.3 - 53.5) without amikacin (section "a" in S2 Table, in bold and italics) and 60.5% (95% CI: 53.3 - 67.8) with amikacin (section "b" in S2 Table, in bold and italics) at 72 h, $p = 0.006$.

Discussion

The objective of this study was to characterise the growth dynamics and virulence of *M. abscessus* clinical strains, with a particular focus on those isolated from CF patients. We aimed to compare the infection kinetics and proliferation capacities of S and R *M. abscessus* strains

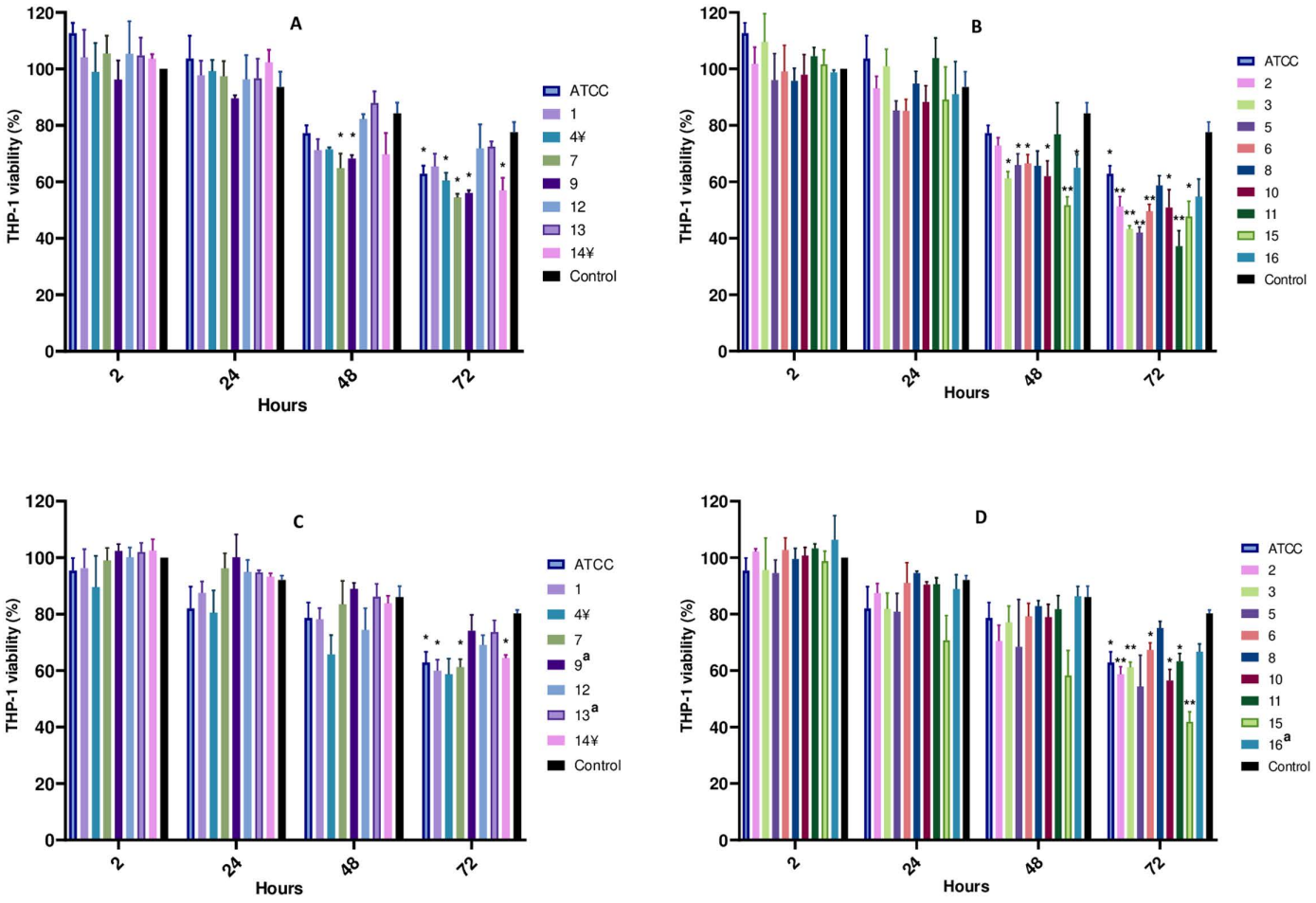

Fig 6. Impact of MABS strains on THP-1 cell viability under untreated and amikacin-treated conditions. Viability percentages are shown relative to the uninfected control at 2 hpi, allowing for the observation of natural viability loss in uninfected THP-1 cells up to 72 hours. Statistical analyses compared the viability of THP-1 cells infected with each strain to the corresponding control at each time point. A, B: Viability of THP-1 cells infected with smooth and rough strains, respectively, in the absence of amikacin. C, D: Viability of THP-1 cells infected with smooth and rough strains, respectively, in the presence of amikacin. Error bars indicate the SD, based on the results from three independent experiments. Two-way ANOVA with Dunnett's post hoc test. * $p < 0.05$, ** $p < 0.01$. [a] Amikacin-resistant strains (numbers 9, 13 and 16) were excluded from this statistical analysis. ¥ Strains exhibiting mixed morphology.

https://doi.org/10.1371/journal.pone.0319710.g006

within THP-1 cells under various experimental conditions. Additionally, we sought to optimise and identify the limitations of the methodologies employed, including the assessment of the impact of amikacin on infection experiments.

We found that nearly 11% of patients had at least one MABS isolate during the study period. Regarding demographic data, the group with MABS isolates was younger than the group without. The difference was marginally significant ($p = 0.049$), but it could suggest that younger individuals might be more susceptible to MABS or more frequently exposed in our setting. In the literature, it is commonly described that CF patients with MABS isolates are younger than those with isolates of other NTM, but it is not usual for them to be younger than groups without NTM isolation [5,28,29]. As for sex, 75.0% (12/16) of the patients with MABS isolation were male. Although the association between sex and MABS isolation was not statistically significant, the higher percentage of male patients with MABS isolation in our study is noteworthy. Nonetheless, in other CF epidemiology studies, either no sex-related differences have been found [5] or, in some cases, a higher prevalence in females has been reported [30]. However, few studies specifically examine the epidemiology of MABS in CF patients, and most of them focus on NTM infections in the general population or a mix of patients with various diseases other than CF [31,32]. Therefore, this observed trend favouring females in NTM infections may not necessarily apply to the CF patient population. These discrepancies call for further investigation to understand the potential role of sex and age in MABS infection dynamics and to clarify these findings.

We observed that 50% of the isolates were R, 37.5% were S, and 12.5% exhibited a mixed morphology, which is consistent with findings from a similar study conducted in Germany [33]. MABSa accounted for most isolates in our study (81.3%), with no MABSb strains identified. This agrees with global data, where MABSa is commonly reported as the most prevalent subspecies, followed by MABSm, while MABSb is infrequently found. Nonetheless, our findings show a higher proportion of MABSa than that of typically reported [34].

Regarding susceptibility testing, we observed high *in vitro* resistance rates (>85%) to doxycycline, tobramycin, ciprofloxacin and moxifloxacin (75%) consistent with findings from previous studies [23,35,36]. Cotrimoxazole also displayed high resistance rates, however, compared to an epidemiological study from our region [23], the present study showed notably lower resistance rates to cotrimoxazole (56.3% vs. 82.3%). Conversely, we identified a considerably higher resistance rate to amikacin (18.8% vs. 2.1%), a finding that also contrasts with most studies where amikacin resistance rates typically remain around 5% [36–39].

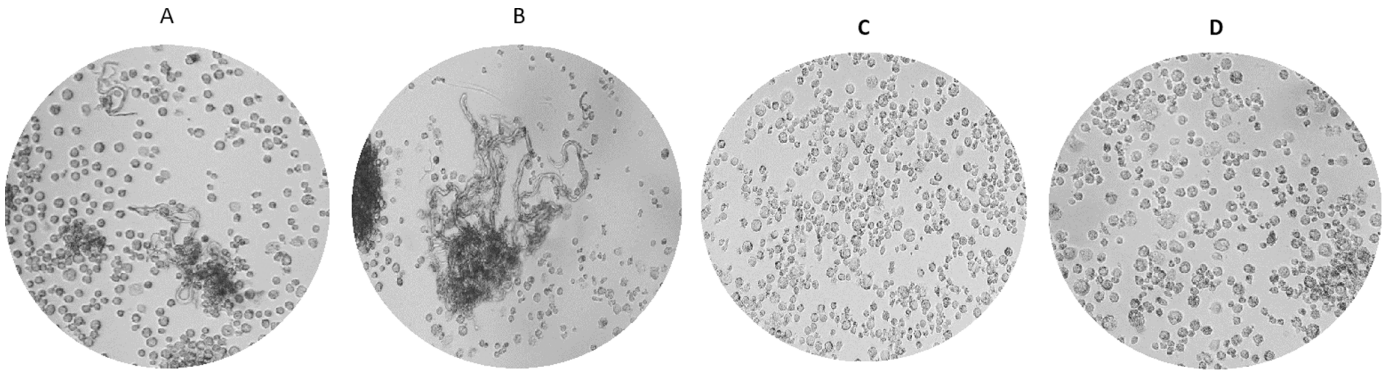

Fig 7. Example of cord-like aggregates produced by the rough strain number 15 at 48 hpi (A) and 72 hpi (B) in the experiment without amikacin. These cords were not observed in smooth strains at 48 hpi (C) or 72 hpi (D).

https://doi.org/10.1371/journal.pone.0319710.g007

These differences may be attributed to the fact that the present study exclusively focused on CF patients, who have different host characteristics and are typically more frequently exposed to different antimicrobial treatments. The 68.8% of strains exhibited either inducible (10 MABSa) or acquired (1 MABSm) macrolide resistance. This high percentage of resistance is attributed to the large proportion of MABSa isolates, which are known to commonly express inducible resistance to macrolides due to the presence of the *erm*(41) gene [8]. These results are particularly concerning since clarithromycin and amikacin are key drugs used in the treatment of MABS infections [12]. We found the lowest resistance rates to imipenem (12.5%), linezolid (6.3%) and cefoxitin (0%), consistent with previous results in our region, although imipenem resistance was significantly lower than typically reported [36–38]. Finally, tigecycline has proven effective *in vitro* against RG-NTM and is currently recommended for treating MABS infections according to existing guidelines (11, 38). Despite the absence of an established susceptibility breakpoint, tigecycline showed strong *in vitro* activity against all isolates, with MICs ≤ 0.5 μg/mL.

Next, we studied growth kinetics and found that S or R strains followed a similar pattern. However, S strains reached significantly higher maximum OD values compared to R strains, especially at later time points. This discrepancy could be due to more pronounced aggregation phenomena in R strains, particularly at later time points. Notably, unreliable OD results have also been described in other studies involving different mycobacterial species [40,41] including *Mycobacterium tuberculosis*, also recognised for its tendency to form aggregates [42]. Despite efforts to disrupt aggregates by shaking with glass beads and syringe passages, R strain cultures remained less homogeneous. The bacterial aggregation led to an underestimation of OD measurements, making the CFU-OD = 1 ratio unreliable for establishing a known bacterial inoculum, especially for R strains. The doubling time observed for S (5.3 hours) and R strains (5.5 hours) were nearly identical, and very similar to those reported in a previous study utilising S and R laboratory strains [43]. These similarities reinforce the conclusion that the elevated CFU-OD = 1 ratio observed in R strains is attributable to aggregation effects rather than inherent differences in growth rates. After using this method and recounting the CFUs to verify whether the inocula contained the necessary bacterial concentration, it was observed that the concentration ranges obtained were highly variable (median = 7.2×10^5 CFU/mL; range: $1.1 \times 10^4 - 1.2 \times 10^7$). This suggests that procedures such as centrifugation and washing of the broth culture during the logarithmic phase might not be robust enough to maintain a consistent OD-CFU ratio across experiments. Therefore, to ensure accurate and consistent infection inocula, we performed a procedure involving the freezing of aliquots of known concentrations, as performed in previous studies [27,44]. This approach provided robust and reproducible data (median = 9.9×10^5 CFU/mL, range: $7.5 \times 10^5 - 1.3 \times 10^6$), accommodating the unique characteristics and growth phase variations of each strain. Consequently, we selected this method for preparing bacterial inocula for subsequent infection experiments.

When examining intracellular growth by using the THP-1 cell infection model we observed that R strains reached higher CFU/mL compared to S strains at all time points and medium conditions. However, statistically significant differences were observed only at specific time points. In the absence of amikacin, significant differences between R and S strains were observed at both 2 hpi and 72 hpi. A recent study also reported that the proportion of infected macrophages was significantly higher among clinical R strains compared to S strains at 72 hours, though no differences were observed at 4 hpi [45]. Although differences at 24 and 48 hpi were not statistically significant, they were remarkably close to significance. The significant differences observed at 72 hpi could be due to the aggregation and clumping behaviours characteristic of R strains, which formed extracellular cord-like aggregates and persisted adhered to the wells despite several dPBS washes (Fig 7). Additionally, this

fact might allow for the reinternalisation of the mycobacteria, which could more significantly affect macrophage viability in the absence of amikacin, as observed in the viability experiments.

Notably, when using amikacin after infection, significant differences in CFU numbers were only noted at 2 hpi, where R strains showed higher numbers. This suggests that the R morphotype might be more efficiently taken up by macrophages and/or phagocytised in small bacterial aggregates, unlike S strains, which are frequently phagocytised individually, as described previously [43,46]. The observed differences in internalisation indices imply that certain strains have a greater capacity to invade host cells compared to the ATCC reference strain. These variations may impact the capacity of macrophages to eliminate intracellular bacteria. The significantly higher internalisation indices observed in some strains (specially R morphotype) underscore their potential for enhanced pathogenicity, highlighting the need for further investigation into the underlying mechanisms. However, as previously mentioned, some strains deviated from this trend. Strains 4 and 14 displayed a mixed morphology and, despite being predominantly smooth, their internalisation indices were closer to that of rough strains. In contrast, rough strain 8 exhibited a notably low internalisation index. These inconsistencies encourage further investigation to understand why its behaviour differs from that of the other rough strains. In the literature, different internalisation indices have been described depending on experimental conditions such as the duration of cell exposure to infection, the multiplicity of infection or the cells used [46,47], but when comparing S and R internalisation rates, this index is generally higher for R strains [46].

In the THP-1 viability assays, significant differences in THP-1 cell viability were observed when comparing infections with R versus S strains in the amikacin-free experiment at 48 and 72 hpi (Fig 5A and section "a" in S2 Table). Conversely, no statistically significant differences in mean viability were measured in the presence of amikacin (Fig 5B and section "b" in S2 Table). Despite this, several R strains exhibited a more pronounced reduction in THP-1 cell viability at 48 and 72 hpi (without amikacin, Fig 6A and 6B) or at 72h (with amikacin, Fig 6C and 6D), when compared individually to uninfected THP-1 controls. These findings are consistent with previous studies, which also reported that R strains caused higher macrophage death at later time points compared to S strains [46,48]. However, Aulicinio et al. found a strong similarity in transcriptional responses to both morphotypes, while noting a distinct inflammatory response. Specifically, R strains triggered a less pronounced inflammatory reaction, which may facilitate their persistence within macrophages [48].

Finally, when comparing THP-1 cell viability under conditions with and without amikacin within the same morphotype, no significant differences were observed in the impact on THP-1 cell viability when infected with S strains at any time point analysed (Fig 5C), indicating that the presence or absence of amikacin had little effect on viability results in this morphotype. In contrast, R strains showed a significantly greater impact on THP-1 viability at 48 and 72 hpi when amikacin was absent. Specifically, THP-1 viability was reduced by 10.6% ($p = 0.01$) at 48 hpi (Fig 5D and S2 Table, in bold) and by 12.2% ($p = 0.006$) at 72 hpi in the absence of amikacin (Fig 5D and S2 Table, in bold and italics). Overall, the R strains exhibited more significant impact in cell viability, especially in the experiments without amikacin and becomes more evident over time (Figs 5 and 6).

In the context of human infection, these findings highlight the complex dynamics of MABS infections, especially in CF patients. The higher CFU counts and the more significant impact on cell viability observed in the R strains suggest that this morphotype might have an enhanced ability to persist in the host. In real-world CF patients, these more aggressive behaviours of strains with R morphotype could translate into chronic and more difficult-to-treat infections [49]. The tendency of R strains to form extracellular cord-like

aggregates may enhance its persistence in the host, evading both the immune response and antibiotic treatment.

However, the results reported herein should be considered in the light of some limitations. This study was conducted in an *in vitro* model, which does not fully replicate the complexity of human infections. In real patients, numerous factors, such as the overall host's immune response, co-existing pathogens, and the unique environment of the CF lung, influence the course of infection. Therefore, while our results offer valuable insights into potential mechanisms of persistence and resistance in MABS infections, further research is needed to determine how these findings translate to clinical settings and to develop more effective therapeutic strategies for managing these difficult-to-treat infections. Moreover, our findings highlight the limitations of commonly employed cellular infection assays. Using amikacin media to control extracellular growth ensures that colony quantification post-lysis reflects the intracellular environment. However, this approach underestimates the true infection burden by not taking into consideration the aggregation and extracellular fate of R strains and their enhanced tendency to lyse macrophages and exit into the extracellular medium. On the other hand, omitting amikacin allows for a more comprehensive understanding of bacterial dynamics, including escape and reinternalisation events, but can lead to overgrowth and complicate interpretation due to extracellular aggregates in this *in vitro* infection model. Finally, while this study included 148 patients, the number of MABS isolates was relatively low. This limited sample size may reduce the power to detect significant associations and restricts the generalisability of the findings to other CF populations. Nonetheless, few studies have explored this topic in depth, and published research in the field typically relies on only a few laboratory strains. Therefore, despite the sample size limitation, our study contributes important data to an underexplored area and underscores the need for continued investigation.

In summary, our study highlights the significant prevalence of MABS isolation among CF patients, particularly among younger individuals. The male predominance in MABS cases, although not statistically significant, prompts further epidemiological investigation. We found high resistance rates to several commonly used antibiotics, with both phenotypic and genotypic testing confirming these resistance patterns. Rough MABS strains showed increased aggregation, complicating OD-based quantification, especially over extended periods; therefore, we recommend preparing frozen aliquots of known concentration to ensure the robustness of such experiments. Most rough strains demonstrated enhanced pathogenicity compared to smooth strains, as evidenced by higher intracellular CFU counts and greater impact on THP-1 cell viability, especially in the absence of amikacin. The differences observed between both methodologies underscore the importance of evaluating results while considering the limitations of each. These observations suggest that rough strains may pose a greater threat to patients, highlighting the need for further investigation into the underlying mechanisms and emphasizing the importance of considering these differences in clinical management. It is also important to note that the genomic characterization of the strains and patient treatment outcomes are still being collected and will be reported once all patient visits have concluded.

Supporting information

S1 Fig. Fluorescence microscopy images at each time point. Representative fluorescence microscopy images of viability of uninfected cells (A, D), cells infected with a rough strain (B, E), and cells infected with a smooth strain (C, F) at each studied time point. Panels A-C show cells non treated with amikacin, while panels D-F show cells treated with amikacin.
(DOCX)

S2 Fig. Relationship between intracellular Mycobacterium abscessus growth and THP-1 cell viability over time under amikacin or amikacin-free conditions. This figure displays the intracellular bacterial burden of Mycobacterium abscessus in THP-1 cells, measured as CFU/mL, along with the corresponding THP-1 cell viability over time. The left axis and data points represent the mean CFU/mL (log scale) of triplicates. The right axis and bars represent the percentage of THP-1 cell viability relative to the 2h non-infected control at each time point post-infection, expressed as the mean ± standard deviation of triplicates. **A, B:** data for smooth and rough strains, respectively, in the absence of amikacin. **C, D**: data for smooth and rough strains, respectively, in the presence of amikacin. ¥ Strains exhibiting mixed morphology.
(DOCX)

S1 Table. Mean bacterial doubling time by strain and by morphology.
(DOCX)

S2 Table. Viability of THP-1 cells infected with S and R strains under amikacin and amikacin-free conditions.
(DOCX)

Acknowledgments

We thank members of the Department of Biochemistry, School of Medicine, Universidad Autónoma de Madrid, Madrid, Spain: Bruno Sainz Anding; Sonia Alcalá Sánchez; Diego Navarro Vera; Juan Carlos López Gil; Laura Ruiz Cañas; Adrián Palencia Campos; Sandra Batres Ramos for lending us the fluorescence microscope and for their assistance in using it.

Author contributions

Conceptualization: Alba Ruedas-López, Rafael Prados-Rosales, Paula López-Roa.

Data curation: Alba Ruedas-López, Marta Tato, Paula López-Roa.

Formal analysis: Alba Ruedas-López, Rafael Prados-Rosales, Paula López-Roa.

Funding acquisition: Rafael Prados-Rosales, Paula López-Roa.

Investigation: Alba Ruedas-López, Marta Tato, Laura Lerma, Rafael Prados-Rosales, Paula López-Roa.

Methodology: Alba Ruedas-López, Marta Tato, Laura Lerma, Rafael Prados-Rosales, Paula López-Roa.

Project administration: Alba Ruedas-López, Rafael Prados-Rosales, Paula López-Roa.

Resources: Alba Ruedas-López, Marta Tato, Jaime Esteban, María-Carmen Muñoz-Egea, Carlos Toro, Diego Domingo, Rafael Prados-Rosales, Paula López-Roa.

Supervision: Rafael Prados-Rosales, Paula López-Roa.

Validation: Alba Ruedas-López, Rafael Prados-Rosales, Paula López-Roa.

Visualization: Alba Ruedas-López.

Writing – original draft: Alba Ruedas-López, Rafael Prados-Rosales, Paula López-Roa.

Writing – review & editing: Alba Ruedas-López, Marta Tato, Laura Lerma, Jaime Esteban, María-Carmen Muñoz-Egea, Carlos Toro, Diego Domingo, Rafael Prados-Rosales, Paula López-Roa.

References

1. Scollan ME, Kwinta B, Aaron J, Gallitano S. An institutional series of skin and soft tissue infections due to rapidly growing mycobacteria. J Am Acad Dermatol. 2024;91(4):722–4. https://doi.org/10.1016/j.jaad.2024.05.070 PMID: 38844008
2. Furuya EY, Paez A, Srinivasan A, Cooksey R, Augenbraun M, Baron M, et al. Outbreak of Mycobacterium abscessus wound infections among "lipotourists" from the United States who underwent abdominoplasty in the Dominican Republic. Clin Infect Dis. 2008;46(8):1181–8. https://doi.org/10.1086/529191 PMID: 18444853
3. Jeong YJ, Lee KS, Koh W-J, Han J, Kim TS, Kwon OJ. Nontuberculous mycobacterial pulmonary infection in immunocompetent patients: comparison of thin-section CT and histopathologic findings. Radiology. 2004;231(3):880–6. https://doi.org/10.1148/radiol.2313030833 PMID: 15118112
4. Swenson C, Zerbe CS, Fennelly K. Host variability in NTM disease: implications for research needs. Front Microbiol. 2018;9:2901. https://doi.org/10.3389/fmicb.2018.02901 PMID: 30559727
5. Marshall JE, Mercaldo RA, Lipner EM, Prevots DR. Incidence of nontuberculous mycobacteria infections among persons with cystic fibrosis in the United States (2010-2019). BMC Infect Dis. 2023;23(1):489. https://doi.org/10.1186/s12879-023-08468-6 PMID: 37488500
6. Floto RA, Olivier KN, Saiman L, Daley CL, Herrmann J-L, Nick JA, et al. US Cystic Fibrosis Foundation and European Cystic Fibrosis Society consensus recommendations for the management of non-tuberculous mycobacteria in individuals with cystic fibrosis: executive summary. Thorax. 2016;71(1):88–90. https://doi.org/10.1136/thoraxjnl-2015-207983 PMID: 26678435
7. Tortoli E, Kohl TA, Brown-Elliott BA, Trovato A, Leão SC, Garcia MJ, et al. Emended description of Mycobacterium abscessus, Mycobacterium abscessus subsp. abscessus and Mycobacteriumabscessus subsp. bolletii and designation of Mycobacteriumabscessus subsp. massiliense comb. nov. Int J Syst Evol Microbiol. 2016;66(11):4471–9. https://doi.org/10.1099/ijsem.0.001376 PMID: 27499141
8. Nash KA, Brown-Elliott BA, Wallace RJ Jr. A novel gene, erm(41), confers inducible macrolide resistance to clinical isolates of Mycobacterium abscessus but is absent from Mycobacterium chelonae. Antimicrob Agents Chemother. 2009;53(4):1367–76. https://doi.org/10.1128/AAC.01275-08 PMID: 19171799
9. Pawlik A, Garnier G, Orgeur M, Tong P, Lohan A, Le Chevalier F, et al. Identification and characterization of the genetic changes responsible for the characteristic smooth-to-rough morphotype alterations of clinically persistent Mycobacterium abscessus. Mol Microbiol. 2013;90(3):612–29. https://doi.org/10.1111/mmi.12387 PMID: 23998761
10. Rhoades ER, Archambault AS, Greendyke R, Hsu F-F, Streeter C, Byrd TF. Mycobacterium abscessus Glycopeptidolipids mask underlying cell wall phosphatidyl-myo-inositol mannosides blocking induction of human macrophage TNF-alpha by preventing interaction with TLR2. J Immunol. 2009;183(3):1997–2007. https://doi.org/10.4049/jimmunol.0802181 PMID: 19596998
11. Touré H, Galindo LA, Lagune M, Glatigny S, Waterhouse RM, Guénal I, et al. Mycobacterium abscessus resists the innate cellular response by surviving cell lysis of infected phagocytes. PLoS Pathog. 2023;19(3):e1011257. https://doi.org/10.1371/journal.ppat.1011257 PMID: 36972320
12. Daley CL, Iaccarino JM, Lange C, Cambau E, Wallace RJ Jr, Andrejak C, et al. Treatment of nontuberculous mycobacterial pulmonary disease: an official ATS/ERS/ESCMID/IDSA clinical practice guideline. Eur Respir J. 2020;56(1):2000535. https://doi.org/10.1183/13993003.00535-2020 PMID: 32636299
13. Byrd TF, Lyons CR. Preliminary characterization of a Mycobacterium abscessus mutant in human and murine models of infection. Infect Immun. 1999;67(9):4700–7. https://doi.org/10.1128/IAI.67.9.4700-4707.1999 PMID: 10456919
14. Belisle JT, Brennan PJ. Chemical basis of rough and smooth variation in mycobacteria. J Bacteriol. 1989;171(6):3465–70. https://doi.org/10.1128/jb.171.6.3465-3470.1989 PMID: 2722755
15. Howard ST, Rhoades E, Recht J, Pang X, Alsup A, Kolter R, et al. Spontaneous reversion of Mycobacterium abscessus from a smooth to a rough morphotype is associated with reduced expression of glycopeptidolipid and reacquisition of an invasive phenotype. Microbiology (Reading). 2006;152(Pt 6):1581–90. https://doi.org/10.1099/mic.0.28625-0 PMID: 16735722
16. Catherinot E, Clarissou J, Etienne G, Ripoll F, Emile J-F, Daffé M, et al. Hypervirulence of a rough variant of the Mycobacterium abscessus type strain. Infect Immun. 2007;75(2):1055–8. https://doi.org/10.1128/IAI.00835-06 PMID: 17145951
17. Jönsson BE, Gilljam M, Lindblad A, Ridell M, Wold AE, Welinder-Olsson C. Molecular epidemiology of mycobacterium abscessus, with focus on cystic fibrosis. J Clin Microbiol. 2007;45(5):1497–504. https://doi.org/10.1128/JCM.02592-06 PMID: 17376883

18. Tsuchiya S, Yamabe M, Yamaguchi Y, Kobayashi Y, Konno T, Tada K. Establishment and characterization of a human acute monocytic leukemia cell line (THP-1). Int J Cancer. 1980;26(2):171–6. https://doi.org/10.1002/ijc.2910260208 PMID: 6970727

19. Matsumoto Y, Fukano H, Hasegawa N, Hoshino Y, Sugita T. Quantitative evaluation of Mycobacterium abscessus clinical isolate virulence using a silkworm infection model. PLoS One. 2022;17(12):e0278773. https://doi.org/10.1371/journal.pone.0278773 PMID: 36538550

20. Rose SJ, Neville ME, Gupta R, Bermudez LE. Delivery of aerosolized liposomal amikacin as a novel approach for the treatment of nontuberculous mycobacteria in an experimental model of pulmonary infection. PLoS One. 2014;9(9):e108703. https://doi.org/10.1371/journal.pone.0108703 PMID: 25264757

21. Rampacci E, Stefanetti V, Passamonti F, Henao-Tamayo M. Preclinical models of nontuberculous mycobacteria infection for early drug discovery and vaccine research. Pathogens. 2020;9(8):641. https://doi.org/10.3390/pathogens9080641 PMID: 32781698

22. REDCap (Research Electronic Data Capture). Available from: https://projectredcap.org/

23. Ruedas-López A, Tato M, Broncano-Lavado A, Esteban J, Ruiz-Serrano MJ, Sánchez-Cueto M, et al. Subspecies distribution and antimicrobial susceptibility testing of mycobacterium abscessus clinical isolates in Madrid, Spain: a retrospective multicenter study. Microbiol Spectr. 2023;11(3):e0504122. https://doi.org/10.1128/spectrum.05041-22 PMID: 37212700

24. CLSI. Susceptibility testing of Mycobacteria, Nocardia spp., and other aerobic Actinomycetes. 3rd ed. CLSI standard M24. Wayne (PA): Clinical and Laboratory Standard Institute; 2018.

25. Moore M, Frerichs JB. An unusual acid-fast infection of the knee with subcutaneous, abscess-like lesions of the gluteal region; report of a case with a study of the organism, Mycobacterium abscessus, n. sp. J Invest Dermatol. 1953;20(2):133–69. https://doi.org/10.1038/jid.1953.18 PMID: 13035193

26. Schneider CA, Rasband WS, Eliceiri KW. NIH Image to ImageJ: 25 years of image analysis. Nat Methods. 2012;9(7):671–5. https://doi.org/10.1038/nmeth.2089 PMID: 22930834

27. Molina-Torres CA, Tamez-Peña L, Castro-Garza J, Ocampo-Candiani J, Vera-Cabrera L. Evaluation of the intracellular activity of drugs against Mycobacterium abscessus using a THP-1 macrophage model. J Microbiol Methods. 2018;148:29–32. https://doi.org/10.1016/j.mimet.2018.03.020 PMID: 29626567

28. Catherinot E, Roux A-L, Vibet M-A, Bellis G, Ravilly S, Lemonnier L, et al. Mycobacterium avium and Mycobacterium abscessus complex target distinct cystic fibrosis patient subpopulations. J Cyst Fibros. 2013;12(1):74–80. https://doi.org/10.1016/j.jcf.2012.06.009 PMID: 22857820

29. Olivier KN, Weber DJ, Wallace RJ Jr, Faiz AR, Lee J-H, Zhang Y, et al. Nontuberculous mycobacteria. I: multicenter prevalence study in cystic fibrosis. Am J Respir Crit Care Med. 2003;167(6):828–34. https://doi.org/10.1164/rccm.200207-678OC PMID: 12433668

30. Roux A-L, Catherinot E, Ripoll F, Soismier N, Macheras E, Ravilly S, et al. Multicenter study of prevalence of nontuberculous mycobacteria in patients with cystic fibrosis in france. J Clin Microbiol. 2009;47(12):4124–8. https://doi.org/10.1128/JCM.01257-09 PMID: 19846643

31. Winthrop KL, McNelley E, Kendall B, Marshall-Olson A, Morris C, Cassidy M, et al. Pulmonary nontuberculous mycobacterial disease prevalence and clinical features: an emerging public health disease. Am J Respir Crit Care Med. 2010;182(7):977–82. https://doi.org/10.1164/rccm.201003-0503OC PMID: 20508209

32. Griffith DE, Girard WM, Wallace Jr RJ. Clinical features of pulmonary disease caused by rapidly growing mycobacteria. An analysis of 154 patients. Am Rev Respir Dis. 1993;147(5):1271–8. https://doi.org/10.1164/ajrccm/147.5.1271 PMID: 8484642

33. Rüger K, Hampel A, Billig S, Rücker N, Suerbaum S, Bange F-C. Characterization of rough and smooth morphotypes of Mycobacterium abscessus isolates from clinical specimens. J Clin Microbiol. 2014;52(1):244–50. https://doi.org/10.1128/JCM.01249-13 PMID: 24197890

34. Koh W-J, Stout JE, Yew W-W. Advances in the management of pulmonary disease due to Mycobacterium abscessus complex. Int J Tuberc Lung Dis. 2014;18(10):1141–8. https://doi.org/10.5588/ijtld.14.0134 PMID: 25216826

35. Chua KYL, Bustamante A, Jelfs P, Chen SC-A, Sintchenko V. Antibiotic susceptibility of diverse Mycobacterium abscessus complex strains in New South Wales, Australia. Pathology. 2015;47(7):678–82. https://doi.org/10.1097/PAT.0000000000000327 PMID: 26517625

36. Sukmongkolchai S, Petsong S, Oudomying N, Prommi A, Payungporn S, Usawakidwiree W, et al. Clinical characteristics and drug susceptibility profiles of Mycobacterium abscessus complex infection at a medical school in Thailand. Ann Clin Microbiol Antimicrob. 2023;22(1):87. https://doi.org/10.1186/s12941-023-00637-4 PMID: 37735687

37. Teri A, Sottotetti S, Arghittu M, Girelli D, Biffi A, D'Accico M, et al. Molecular characterization of Mycobacterium abscessus subspecies isolated from patients attending an Italian Cystic Fibrosis Centre. New Microbiol. 2020;43(3):127–32. PMID: 32656572

38. Cho EH, Huh HJ, Song DJ, Lee SH, Kim CK, Shin SY, et al. Drug susceptibility patterns of Mycobacterium abscessus and Mycobacterium massiliense isolated from respiratory specimens. Diagn Microbiol Infect Dis. 2019;93(2):107–11. https://doi.org/10.1016/j.diagmicrobio.2018.08.008 PMID: 30236529

39. Guo Q, Wei J, Zou W, Li Q, Qian X, Zhu Z. Antimicrobial susceptibility profiles of Mycobacterium abscessus complex isolates from respiratory specimens in Shanghai, China. J Glob Antimicrob Resist. 2021;25:72–6. https://doi.org/10.1016/j.jgar.2021.02.024 PMID: 33689828

40. Kralik P, Beran V, Pavlik I. Enumeration of Mycobacterium avium subsp. paratuberculosis by quantitative real-time PCR, culture on solid media and optical densitometry. BMC Res Notes. 2012;5:114. https://doi.org/10.1186/1756-0500-5-114 PMID: 22357065

41. Lambrecht RS, Carriere JF, Collins MT. A model for analyzing growth kinetics of a slowly growing Mycobacterium sp. Appl Environ Microbiol. 1988;54(4):910–6. https://doi.org/10.1128/aem.54.4.910-916.1988 PMID: 3377502

42. Peñuelas-Urquides K, Villarreal-Treviño L, Silva-Ramírez B, Rivadeneyra-Espinoza L, Said-Fernández S, de León MB. Measuring of Mycobacterium tuberculosis growth. A correlation of the optical measurements with colony forming units. Braz J Microbiol. 2013;44(1):287–9. https://doi.org/10.1590/S1517-83822013000100042 PMID: 24159318

43. Roux A-L, Viljoen A, Bah A, Simeone R, Bernut A, Laencina L, et al. The distinct fate of smooth and rough Mycobacterium abscessus variants inside macrophages. Open Biol. 2016;6(11):160185. https://doi.org/10.1098/rsob.160185 PMID: 27906132

44. Mariotti S, Pardini M, Teloni R, Gagliardi MC, Fraziano M, Nisini R. A method permissive to fixation and permeabilization for the multiparametric analysis of apoptotic and necrotic cell phenotype by flow cytometry. Cytometry A. 2017;91(11):1115–24. https://doi.org/10.1002/cyto.a.23268 PMID: 29072808

45. Pichler V, Dalkilic L, Shoaib G, Shapira T, Rankine-Wilson L, Boudehen Y-M, et al. The diversity of clinical Mycobacterium abscessus isolates in morphology, glycopeptidolipids and infection rates in a macrophage model. 2024.

46. Brambilla C, Llorens-Fons M, Julián E, Noguera-Ortega E, Tomàs-Martínez C, Pérez-Trujillo M, et al. Mycobacteria clumping increase their capacity to damage macrophages. Front Microbiol. 2016;7:1562. https://doi.org/10.3389/fmicb.2016.01562 PMID: 27757105

47. Bettencourt P, Carmo N, Pires D, Timóteo P, Anes E. Mycobacterial infection of macrophages: the effect of the multiplicity of infection. In: Antimicrobial research: novel bioknowledge and educational programs. Formatex Research Center; 2017.

48. Aulicino A, Dinan AM, Miranda-CasoLuengo AA, Browne JA, Rue-Albrecht K, MacHugh DE, et al. High-throughput transcriptomics reveals common and strain-specific responses of human macrophages to infection with Mycobacterium abscessus Smooth and Rough variants. BMC Genomics. 2015;16:1046. https://doi.org/10.1186/s12864-015-2246-1 PMID: 26654095

49. Parmar S, Tocheva EI. The cell envelope of Mycobacterium abscessus and its role in pathogenesis. PLoS Pathog. 2023;19(5):e1011318. https://doi.org/10.1371/journal.ppat.1011318 PMID: 37200238